AWARD NUMBER: W81XWH-09-1-0498

TITLE: Measuring Blast-Related Intracranial Pressure Within the Human Head

PRINCIPAL INVESTIGATOR: Cynthia Bir

CONTRACTING ORGANIZATION: Wayne State University
Detroit, MI 48202

REPORT DATE: February 2011

TYPE OF REPORT: Final

PREPARED FOR: U.S. Army Medical Research and Materiel Command
Fort Detrick, Maryland 21702-5012

DISTRIBUTION STATEMENT: Approved for Public Release;
Distribution Unlimited

REPORT DOCUMENTATION PAGE

Form Approved
OMB No. 0704-0188

1. REPORT DATE	**2. REPORT TYPE**	**3. DATES COVERED**
1 February 2011	Final	1 Aug 2009 – 31 Jan 2011

4. TITLE AND SUBTITLE

Measuring Blast-Related Intracranial Pressure Within the Human Head

5a. CONTRACT NUMBER

5b. GRANT NUMBER
W81XWH-09-1-0498

5c. PROGRAM ELEMENT NUMBER

6. AUTHOR(S)

Cynthia Bir

E-Mail: cbir@wayne.edu

5d. PROJECT NUMBER

5e. TASK NUMBER

5f. WORK UNIT NUMBER

7. PERFORMING ORGANIZATION NAME(S) AND ADDRESS(ES)
Wayne State University
Detroit, MI 48202

8. PERFORMING ORGANIZATION REPORT NUMBER

9. SPONSORING / MONITORING AGENCY NAME(S) AND ADDRESS(ES)
U.S. Army Medical Research and Materiel Command
Fort Detrick, Maryland 21702-5012

10. SPONSOR/MONITOR'S ACRONYM(S)

11. SPONSOR/MONITOR'S REPORT NUMBER(S)

12. DISTRIBUTION / AVAILABILITY STATEMENT
Approved for Public Release; Distribution Unlimited

13. SUPPLEMENTARY NOTES

14. ABSTRACT

The goal of this research effort is to determine the transient responses of the skull-brain system during exposure to blast to help identify the primary mechanism of blast-TBI. The aims of this proposal are (1) to ascertain the relationship between magnitude levels of incident pressure and values of intracranial pressure, surface strain, and kinematic response, (2) to investigate the effects of orientation on all three parameters, and (3) to compare pressure distribution patterns with a finite element model. Preliminary data indicate there are significant factors of paramount importance when performing ICP-PMHS testing: sensor location in the brain, exposure at blast, orientation of head and magnitude of the blast.

15. SUBJECT TERMS
Cadaver, blast neurotrauma, intra-cranial pressure

16. SECURITY CLASSIFICATION OF:			**17. LIMITATION OF ABSTRACT**	**18. NUMBER OF PAGES**	**19a. NAME OF RESPONSIBLE PERSON**
a. REPORT	**b. ABSTRACT**	**c. THIS PAGE**			USAMRMC
U	U	U	UU	25	**19b. TELEPHONE NUMBER** *(include area code)*

Standard Form 298 (Rev. 8-98)
Prescribed by ANSI Std. Z39.18

Table of Contents

INTRODUCTION

The goal of this research effort is to determine the transient responses of the skull-brain system during exposure to blast to help identify the primary mechanism of blast-TBI. The aims of this proposal are (1) to ascertain the relationship between magnitude levels of incident pressure and values of intracranial pressure, surface strain, and kinematic response, (2) to investigate the effects of orientation on all three parameters, and (3) to compare pressure distribution patterns with a finite element model. The proposed research is *significant* because resolution of the mode of energy transfer and of the induced stresses within the skull-brain system will allow for creations of mitigation/protective techniques/equipment, as well as design of experiments investigating live-cell response using more reliable computer simulated models.

BODY

Since the grant was awarded in August 2009, we have undergone several key experiments in order to accomplish our specific aims. First, we determined linear acceleration values produced at the proposed blast overpressures using an instrumented biomechanical surrogate; the Hybrid III 50^{th} percentile head form. Secondly, we began optimization of specimen preparation and testing procedures to most accurately measure ICP during blast testing. We found that sealing techniques for placement of the ICP sensors in the human skull had to be modified from techniques previously used for animal testing. Third, we began measuring strains from multiple sites of the human skull during blast testing. We found that the techniques for placement of the strain gages needed to be improved to guarantee a dependable adhesion of such gages for the entire duration of the experiment.

An existing finite element model previously validated for blunt impact analysis was modified for the blast loading scenarios. Validation of this model was accomplished using data collected from the experimental work conducted during the first phases on this research.

A detailed description of our methodology, results and challenges are presented below.

Wayne State University shock wave generator (WSU-SWG).

To simulate a free field blast wave in the laboratory, the Bioengineering Center at Wayne State University houses a shock wave generator (Figure 1) activated by compressed helium. A shock wave generator is a tube consisting of two separate chambers: the driver, where the pressured gas is inserted by means of compressor system, and the driven, where the shock wave propagates (Celander et al. 1955). In the simplest shock tube operation, the driver is separated from the driven by a frangible membrane. For any given material the membrane ruptures at a particular pressure that is directly proportional to its thickness and allows the generation of the shock wave into the driven. (Note: because the wave is produced by compressed gas bursting a membrane instead of an actual chemical explosion, we use the term blast simulation instead of blast and shock wave instead of blast wave.) The test section usually contains air at atmospheric pressure before the bursting of the diaphragm. If the diaphragm bursts ideally, a uniform shock front quickly develops and propagates down the test section.

The WSU SWG had been used previously to conduct testing using a rodent model. In an effort to accommodate the larger cephalic specimens, an expansion section was built. This expansion section was carefully design to create the ideal wave profile without refractions and is 14 feet in length (complete SWG length is 26 feet). At the specimen position, which is inside the expansion, it measures 30 inches in diameter and can accommodate the specimens to be placed in the primary blast wave with adequate air flow around all sides.

The incident shock wave overpressure values provided for the PMHS tests were approximately 12.5, 17, and 20 psi (86.2, 117.2, 137.9 kPa) in magnitude. These pressure values were measured by a probe placed at the site where the specimen was to be positioned approximately 49 inches from the open end of the tube. The probe contains pressure gages that measure the static and stagnation pressures; stagnation pressure, also called incident pressure, can be considered a good approximation of static and dynamic pressures combined, and subsequent data processing allows calculation of dynamic pressures.

Calibration of the WSU SWG determined that the generated pressure waveforms have a decaying profile credibly similar to that of the positive phase of the free field blast (Figure 2). However, it is very important to note that not all zones within the shock tube are appropriate for blast simulation: at some locations within the tube, the effects of anomalous flow features are exaggerated and will corrupt the experimental conditions sooner than in other locations. Hybrid III and human specimen were consistently placed at 49 inches from the open end of the tube, where conditions were deemed optimal for simulation of the positive phase of the free field blast wave based on wave diagram studies conducted.

Figure 1: Wayne State University shock wave generator

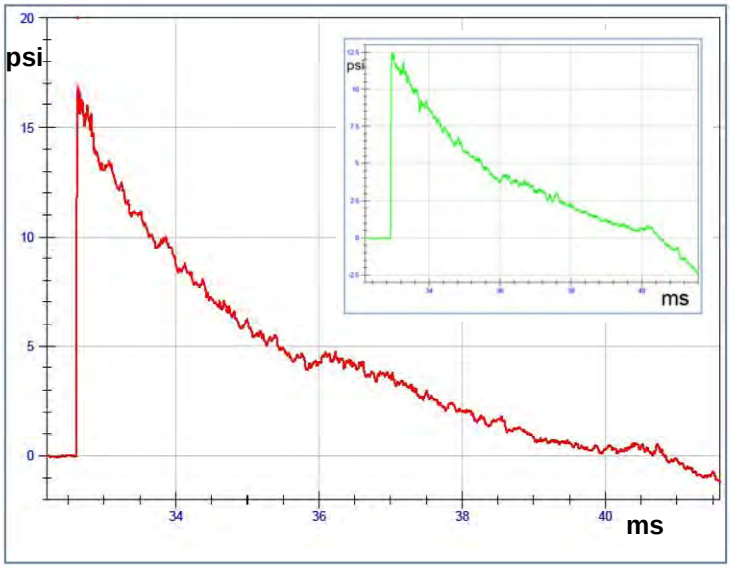

In this example the peak stagnation pressure was around 17 psi (117 kPa) and the positive phase duration was 8 ms.

<u>Insert</u>: Corresponding static pressure profile for the same test. Peak static pressure was around 12.5 psi (86kPa) and the positive phase duration was around 7.5 ms.
The dynamic pressure profile is calculated from such profiles.

Figure 2: Stagnation pressure profile collected near the location where samples are placed for testing.

Pressure sensors

Commercially available sensors from Endevco (models 8515C and 8530C), FISO Technologies (FOP-MIV model) and PCB Piezotronics (102A06 model), were used at the specimen site and along the tube to record the incident shock wave overpressure and the intracranial pressure (ICP) respectively (Figure 3). The sensors differ on several levels according to their purpose. First, the mechanism of measuring pressure is distinctive: sensors used to measure air over-pressure utilize either a piezoresistive or a quartz piezoelectric element to detect sudden change in ambient pressure. They are rugged and able to survive many blast test situations, although they possess high sensitivity and reliability. The monitoring of the ambient overpressure at the target was provided by a pressure probe that contained two Endevco sensors placed frontally and sideon with respect to the shock front.

Sensors used to assess ICP utilize optic technology, measuring pressure by converting wavelength-modulated light into a voltage value. They were designed for medical applications; therefore the sensor is very fragile and weighs only 0.163mg. The tip of the sensor, excluding the connecting optic fiber, measures approximately 0.5mm both in diameter and in length. These characteristics of the sensors are especially important when working in the brain since the sensor should approximate the density of the tissue surrounding it to create as little disturbance as possible. Otherwise, inertia of the sensor may affect the reading of in vivo pressure as intended.

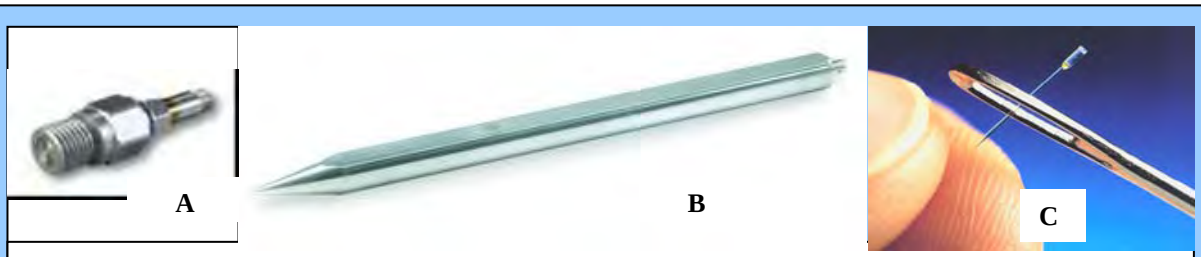

(A) PCB Piezotronics pressure sensor measuring the static component of the shock wave in air along the tube; (B) pressure sensor using Endevco sensor to measure static and stagnation pressures next to the specimen; (C) FISO Technologies optic pressure sensor for intracranial measurements.

Figure 3: Examples of pressure sensors used for shock tests.

Sample preparation

Testing was conducted to assess several key factors and provide future directions. For determining linear acceleration values produced at the proposed blast overpressures, we used an instrumented Hybrid III 50th percentile head form. A tri-axial block of linear accelerometers was placed at the center of gravity of the headform. Data was collected using a TDAS system (DTS, Inc) at 150 kHz.

For the initial testing, we employed an unembalmed PMHS head without a neck, which had been frozen. This was done to save costs and develop all techniques. The remaining four specimens were fresh, unembalmed specimens. For the frozen sample, three FISO optic sensors were implanted in the right frontal cortex, right lateral ventricle, and right parietal lobe and the respective depths of the tip of the sensors from the outer surface of the skull were 25mm, 65mm, and 30mm. Holes were made in the skull using a Dremel rotary tool; each hole (d=1.2mm) had at least three supporting screws that helped hold the sensor in place once inserted (Figure 4A). The FISO sensors were anchored to the skull by using bone cement that adhered to the skull and the screws reinforcing the anchoring site and providing sealing of the hole (Figure 4B).

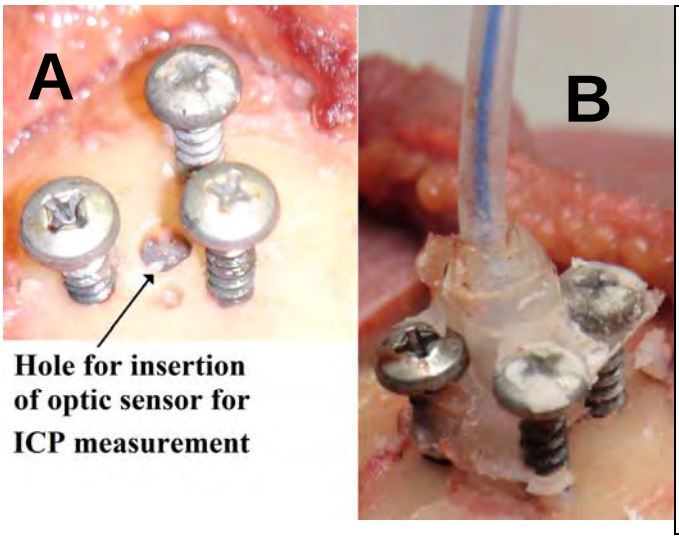

(A) Hole for insertion of optic sensor with supporting screws already in place.
(B) Optic fiber (blue) protected by plastic sheaving, anchored to screws by bone cement. In this picture the cement was partially removed to show the screws underneath. In the actual setup cement is poured in a form that completely encloses the screws and it is left to cure for several minutes. The sheaving on the exposed fiber protects from the blast wind and it is not present on the tract that goes into the brain.

Figure 4: Placement of ICP sensor on the skull

To measure strain, five rosettes were glue to the skull on the left zygomatic bone, the left sphenoid bone, the left parietal bone and the left side of the frontal and occipital bones (20mm on the left side of the midline). The glue adopted was a two part compound: one part was placed on the surface of the skull after a meticulous cleaning and drying process; the second part was placed on the rosette. Once the two parts were pressed together a chemical bond was formed that provided great adhesion. A sealant was also applied on the rosette's exposed surface to avoid contact with bodily fluids that would have altered strain results.

For the remaining four PMHS samples, four FISO optic sensors were implanted in the right frontal cortex, right lateral ventricle, right parietal lobe and right occipital lobe and the respective depths of the tip of the sensors from the outer surface of the skull were 30mm, 30mm, 65mm,

and 30mm. Installation of the pressure sensors and rosettes was performed as previously described.

Note that all pressure sensors were mounted on the right side of the brain, while the five rosettes strain gages were placed on the left side of the skull; this setup was chosen to collect homogeneous data among different locations (see next section).

Experimental setup

To determine the overall kinematics of the event a Hybrid III head form was placed in the tube under two boundary conditions. First it was tested with a Hybrid III neck: an interface plate rigidly mounted the head and neck to the bottom of the expansion tube in the same position along the length of the tub where the PHMS specimens will be placed (Figure 5A). Next the Hybrid head form was mounted without the neck in a soft net that was suspended in the same manner as the PMHS specimens would be during testing (Figure 5B); this was the second boundary condition. For each boundary condition the Hybrid III head form was exposed to several incident shock wave overpressures (target values were 14.5, 17, 20 and 22 psi, which is respectively 100, 117, 138, and 152 kPa); to check for repeatability of results there were at least three tests for each pressure magnitude. Monitoring of the overpressures delivered to the dummies was provided by a pressure probe placed next to the samples. Such probe had pressure gages that could measure the static and stagnation pressures. The head was instrumented with a 3-2-2-2 array of Endevco 7264 accelerometers. The data was collected at 150 KHz with TDAS data acquisition system.

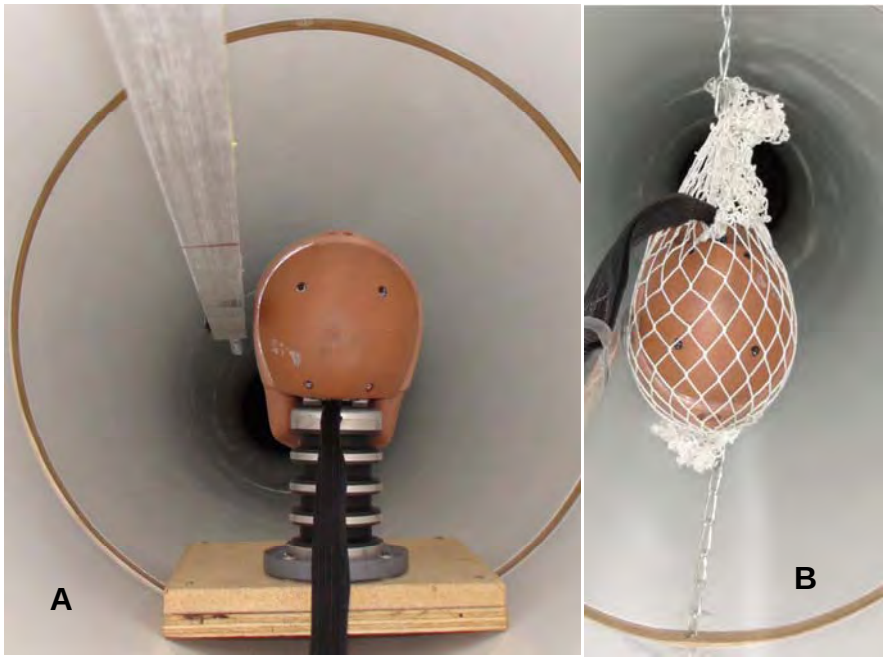

(A) H-III head and neck rigidly mounted on a platform at 49 inches from the open end of the tube.

(B) H-III head inside a soft net suspended at 49 inches from the end of the tube at the location where PMHS specimens will be placed for testing.

The pole next to the dummy both pictures contains the pressure sensors that plot the static and dynamic over-pressures occurring during testing.

Figure 5: Placement of Hybrid III head form under two different boundary conditions.

The PHMS specimen was mounted upside down in a soft net that was suspended in the center of the tube-section at 49 inches from the open end as shown in Figure 5B for the head form. Three target overpressure exposures were chosen: 12.5, 17, and 20 psi. For each target overpressure, a set of five positions were investigated: shockwave hitting frontally (nose facing the blast); shockwave hitting the left side (strain gages facing the blast); shockwave hitting the back of the head; shockwave hitting the right side (pressure sensors facing the blast); then again shockwave hitting frontally (nose facing the blast). The frontal position was repeated at the end of each set to check for reproducibility of results. In fact, due to the harsh environment in which the sensors are required to work, we had to balance the need to maximize the number of successful tests with the necessity to test that results were repeatable.

A total of four fresh, unembalmed specimens were tested (Table 1). All specimens were treated with care and respect based on ethical guidelines established. Approval was obtained from the Wayne State University Human Investigation Committee (HIC) review board prior to the commencement of this study.

Table 1: Post-mortem human specimens tested.

	#2 (WSU 509)	#3 (WSU 510)	#4 (UM 33652)	#5 (UM 33655)
Age	52	87	73	87
Sex	M	F	F	F
Mass (kg)	63.5	49.9	76.6	63.5
Stature (cm)	162.6	160.0	152.4	165.0
Cause of Death	CHF	CHF	CHF	Natural

Task 1 and 2: Determination of the transient response histories of acceleration, intracranial pressure and surface strain values as a function of incident blast strength and investigation of the effect of orientation on all three parameters.

Acceleration

Accelerations generated during blast simulations were measured with an instrumented Hybrid III 50th percentile head form. Originally, these data were to be collected from PMHS specimens. The data collected with the Hybrid III dummy proved that unnecessary. This eliminates test complexity and a test apparatus that could affect results for the other measurements we wanted to collect. A block of accelerometers and angular rate sensors was going to be attached to the skull with screws. This would be a rigid object that could affect strain and/or pressure measurements in the PMHS due to fixation techniques and added mass and rigidity.

The accelerometers were filtered using a CFC1000 filter (-3dB point = 1650 Hz) as described by SAE J211. The acceleration data at the center of gravity (CG) was evaluated using Head Injury Criterion (HIC). The resultant of the 3 accelerometers at the CG was calculated and the HIC calculations computed from this resultant. All acceleration data processing was conducted using Diadem 11.1 (National Instruments). HIC values are provided in Table 2. Also included in this table is the percent risk for MTBI. These values are calculated from a logistic regression curve

created by Zhang et al. (2004). These values are below 10%, which indicates that the conditions studied in our blast overpressure system do not induce injurious linear accelerations.

In combination with the gathering of acceleration data, we collected data regarding the speed of the shock front and the incident and static overpressure values at the specimen's location in 27 tests. Table 3 shows the average speed of the shock front, the average incident overpressure (named **AOP** for Air Over-Pressure), and the average static overpressure for each target pressure.

Table 2: Linear acceleration data from Hybrid III tests

Filename	HIC15	% Risk of MTBI	Target Overpressure
ExpansionTubeTest1	14.84	7.1470	17 psi
ExpansionTubeTest2	19.91	7.5402	17 psi
ExpansionTubeTest3	18.71	7.4454	17 psi
ExpansionTubeTest4	20.17	7.5609	17 psi
ExpansionTubeTest5	21.67	7.6813	17psi
ExpansionTubeTest6	26.80	8.1064	17psi
ExpansionTubeTest7	12.79	6.9935	14.5 psi
ExpansionTubeTest8	11.40	6.8911	14.5 psi
ExpansionTubeTest9	23.46	7.8272	17 psi
ExpansionTubeTest10	9.61	6.7613	14.5 psi
ExpansionTubeTest11	10.26	6.8082	14.5 psi
ExpansionBlastTest12	19.98	7.5458	17 psi
ExpansionBlastTest13	10.70	6.8401	17 psi
ExpansionBlastTest14	9.78	6.7735	17 psi
ExpansionBlastTest15	7.39	6.6035	14.5 psi
ExpansionBlastTest16	9.11	6.7255	14.5 psi
ExpansionBlastTest17	8.71	6.6969	14.5 psi
ExpansionBlastTest18	14.38	7.1123	17 psi
ExpansionBlastTest19	19.17	7.4816	20 psi
ExpansionBlastTest20	32.98	8.6469	20 psi
ExpansionTubeTest21	23.82	7.8569	20 psi
ExpansionBlastTest22	26.62	8.0911	22 psi
ExpansionBlastTest23	31.69	8.5315	22 psi
ExpasionTubeTest24	29.41	8.3308	22 psi

Table 3: Averages for collected data: shock front speed, peak air overpressure (AOP), and peak static overpressure.

TARGET PRESSURE	AVG PEAK AOP PSI (kPa)	AVG FRONT SPEED m/s	AVG PEAK STATIC OP PSI (kPa)
14.5 PSI	13.5 PSI (93kPa)	444.6	10.6 (73.1)
17 PSI	16.3 PSI (112kPa)	459.8	12.6 (86.9)
20 PSI	20.3 PSI (140kPa)	481.7	15.7 (108.3)
22 PSI	22.3 PSI (154kPa)	490.0	15.8 (108.9)

Intracranial Pressure

During 15 blast simulations with each PMHS specimen, pressure data was collected in four different parts of the brain for each PMHS specimen. In each specimen there were 4 optic pressure sensors installed on the anatomical right side of the skull (frontal, ventricle, parietal, occipital). Three pressures (measured sideon, i.e. static pressure) were tested: low (~10psi), medium (~12psi), and high (~15psi). For each pressure, five tests were performed: front exposure, left exposure, back exposure, right exposure, front exposure. Therefore a total of 15 tests for each specimen were carried out. The first and fifth exposures for each pressure group were both front exposures to determine consistency of results (Figure 6).

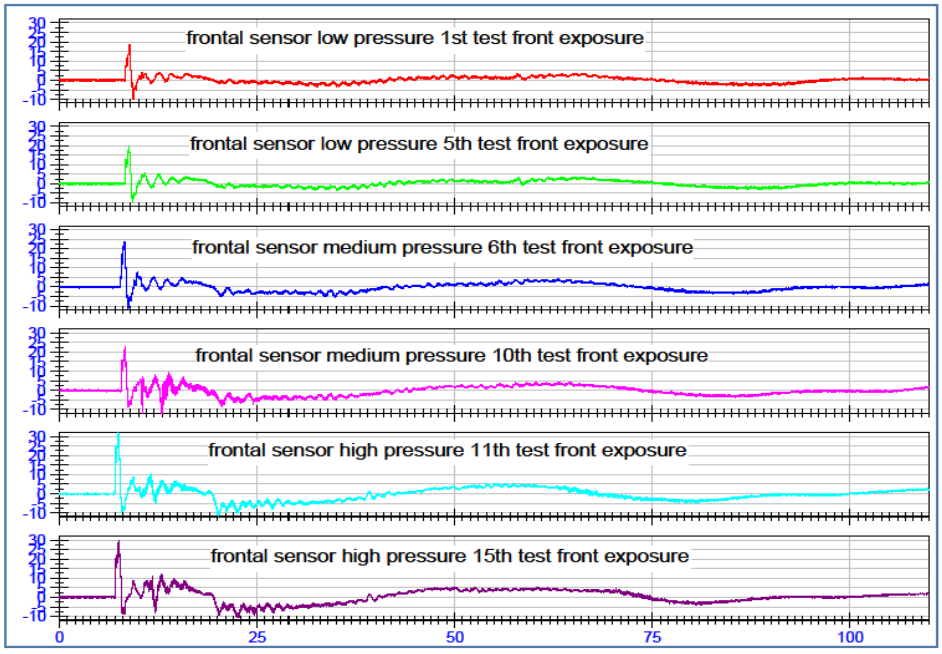

Figure 6: Demonstration of consistent results throughout testing as seen in 1st and 5th frontal exposures.

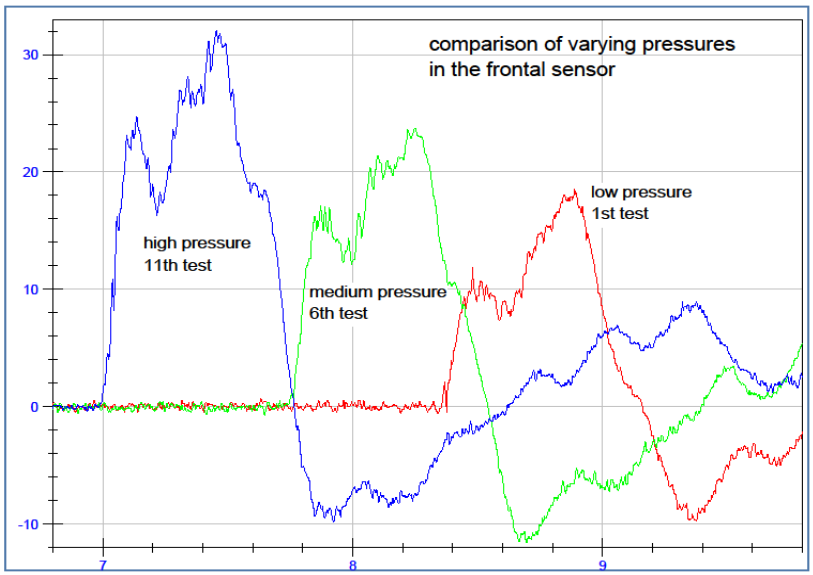

Figure 7: Increased shock wave pressure related in increased ICP.

Figure 7 provides a side by side comparison of the effect of the varying intensity of shock wave pressure on the pressure measured in the frontal lobe. The low sideon pressure (~10 psi) generated approximately 18 psi in the frontal sensor while the medium (~12 psi) and high (~15 psi) generated approximately 22 psi and 32 psi respectively.

In an effort to demonstrate how the pressure wave propagates through the brain, each of the four sensors was observed during a single exposure. Figure 8 demonstrates that during a frontal exposure, the frontal and ventricular sensor experience a positive pressure, whereas the parietal and occipital experience an initial negative pressure. This trend is noted for all specimens and changes depending on orientation of the blast wave.

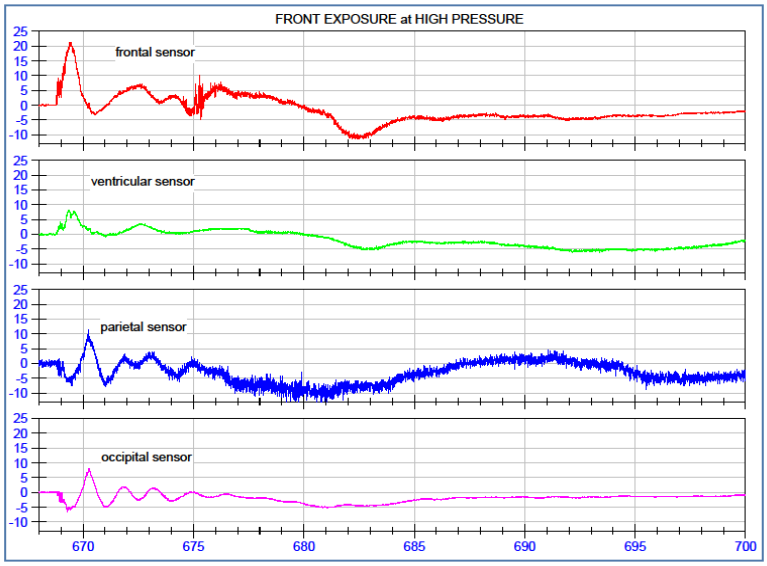

Figure 8: Example of the four pressure sensors with a front exposure.

In order to analyze the pressure measurements, we chose to calculate several key elements of the pressure profiles that we hypothesize may relate to head injury. The **rate of change of pressure** is thought to be an important mechanism of injury. We determined the **first rate** as the first change of pressure (Table 4). This value is not necessarily the highest change of pressure the brain region experienced; in fact another rate, **peak-to-peak rate**, has been provided as an example. The sign in front of the rate indicates increasing compression when positive, and decreasing pressure below ambient when negative. The **pressure differential** was determined, which is an indication of the pressure range endured by the region in the time-window of interest. **Maximum** and **minimum pressures** are also presented separately. These values for each specimen have been determined and tables have been created. Table 4 and Table 5 provide an example of the calculated data from specimen 5.

Table 4: Rate of change of pressure data from cadaver 5 for all three sideon pressure intensities.

Pressure Rates of Change for cadaver-5 (psi/ms)										
	1st rate					peak to peak rate				
ventricle	front 1	right	back	left	front 2	front 1	right	back	left	front 2
10 psi air	**11.18**	**9.7**	**-3.44**	**˜ -7.97**	**9.13**	**-10.09**	**-9.9**	**6.34**	**-9.7**	**-10.37**
12 psi air	**12.43**	**12.44**	**-4.21**	**˜ -7.62**	**15.04**	**-12.48**	**-11.64**	**7.36**	**11.82**	**-8.12**
15 psi air	**20.98**	**14.67**	**-3.67**	**˜ -14.28**	**16.23**	**-14.09**	**-18.49**	**-13.25**	**18.89**	**-19.79**
frontal	front 1	right	back	left	front 2	**front 1**	**right**	**back**	**left**	**front 2**
10 psi air	**36.63**	**10.37**	**-45.76**	**21.8**	**35.64**	**-50.18**	**-22.65**	**30.53**	**-15.38**	**-53.06**
12 psi air	**55.06**	**13.72**	**-58.59**	**32.69**	**56.61**	**-65.1**	**-24.51**	**30.72**	**-28.26**	**-61.4**
15 psi air	**78.98**	**14.16**	**-67.18**	**43.57**	**59.67**	**-77.06**	**-27.3**	**19.36**	**38.63**	**-75.09**
parietal	front 1	right	back	left	front 2	**front 1**	**right**	**back**	**left**	**front 2**
10 psi air	**-3.87**	**21.48**	**29.66**	**-10.69**	**-5.59**	**25.94**	**-16.58**	**-16.75**	**19.63**	**25.95**
12 psi air	**-8.91**	**25.97**	**43.46**	**-13.78**	**-10.82**	**35.04**	**-18.78**	**-24.58**	**15.4**	**35.95**
15 psi air	**-15.75**	**45.48**	**64.55**	**-16.14**	**-9.39**	**60.13**	**-29.3**	**-40.68**	**17.66**	**52.09**
occipital	front 1	right	back	left	front 2	**front 1**	**right**	**back**	**left**	**front 2**
10 psi air	**-3.73**	**5.49**	**4.58**	**-3.45**	**-3.4**	**6.21**	**2.53**	**-1.37**	**5.55**	**7.33**
12 psi air	**-4.37**	**5.29**	**6.1**	**-4.3**	**-5.29**	**8.16**	**6.4**	**-3.94**	**-6.15**	*** 21.75**
15 psi air	**-7.38**	**13.01**	**14.06**	**-6.4**	**-9.69**	*** 33.63**	**14**	**-9.75**	**-10.95**	**20.44**

˜ cable noise that could also be surface-ripples * possible cable noise affecting value

Table 5: ICP data from cadaver 5 for all three sideon pressure intensities.

Differential for cadaver-5										
	peak differential pressure (psi)					time elapsed between peaks (ms)				
ventricle	front 1	right	back	left	front 2	front 1	right	back	left	front 2
10 psi air	**5.55**	**5.04**	**4.39**	**6.01**	**6.43**	**0.788**	**3.24**	**1.02**	**1.15**	**0.816**
12 psi air	**7.99**	**6.09**	**6.36**	**7.54**	**7.27**	**0.852**	**0.888**	**0.864**	**0.844**	**0.896**
15 psi air	**10.71**	**11.77**	**9.43**	**8.72**	**11.31**	**0.76**	**0.744**	**3.72**	**3.54**	**1.14**
frontal	front 1	right	back	left	front 2	front 1	right	back	left	front 2
10 psi air	**25.09**	**7.44**	**16.99**	**9.06**	**26.11**	**0.5**	**3.52**	**2.93**	**0.616**	**0.492**
12 psi air	**31.77**	**9.27**	**20.48**	**12.52**	**30.45**	**0.488**	**0.472**	**1.71**	**1.12**	**4.68**
15 psi air	**37.3**	**13.89**	**26.07**	**21.48**	**33.7**	**0.484**	**1.35**	**2.15**	**0.556**	**0.664**
parietal	front 1	right	back	left	front 2	front 1	right	back	left	front 2
10 psi air	**7.43**	**10.52**	**12.47**	**8.84**	**8.97**	**0.82**	**0.72**	**0.78**	**0.688**	**0.8**
12 psi air	**10.27**	**13.08**	**18.29**	**9.5**	**8.96**	**0.84**	**0.808**	**0.744**	**1.26**	**0.696**
15 psi air	**11.11**	**23.2**	**29.13**	**10.46**	**19.23**	**0.8**	**0.792**	**0.716**	**2.464**	**0.72**
occipital	front 1	right	back	left	front 2	front 1	right	back	left	front 2
10 psi air	**2.72**	**2.25**	**3.53**	**2.31**	**1.46**	**6.12**	**1.74**	**7.48**	**6.24**	**3.04**
12 psi air	**3.04**	**3.12**	**6.24**	**2.09**	**2.62**	**6.98**	**3.92**	**7.44**	**4.548**	**5.36**
15 psi air	**3.14**	**4.76**	**12.49**	**2.72**	**4.77**	**4.74**	**2.45**	**6.63**	**2.476**	**4.04**

Surface Strain

During the series of 15 tests, we collected strain data in five regions of the skull on the PMHS specimens: left zygomatic bone, the left sphenoid bone, the left parietal bone and the left frontal and occipital bones (20 mm from midline). The purpose of a strain gage is to measure the deformations in a given area. Because deformations in materials can be very slight, the sensor has to be very thin so that is does not filter or block specific frequencies of interest. In the methods section, it was discussed that the strain gages were attached to the skull surface by using a two part adhesive that was brushed onto the bone surface, the strain gages were then placed on the adhesive. The technique leads to variations in the amount of adhesive between the sensor surface pad and the skull, which may affect the response of the strain gages. This problem is magnified due to the curvature of the bones of the skull and the highly dynamic pressure environment within the blast tube that can cause the sensors to lose contact with the skull. Therefore additional adhesive was needed to mitigate sensor failure.

It is reasonable to suspect that this buildup of material could have influenced the measured strain signals in this study. Because of this limitation, it is difficult to determine if the measured amplitudes in the data channels are appropriate for quantitative analysis, especially between specimens. The problem is exacerbated because the number of sensors that failed increased as the number of exposures and intensity increased. Thus, complete data sets were rare. Therefore specific results on each PMHS are reported instead of descriptive statistics. Additionally due to the number of strain channels lost during testing, principle strains could not calculated, leading to individual channels analysis. Figure 9 demonstrates the trend that, as pressure intensity increased, the amount of deflection increased.

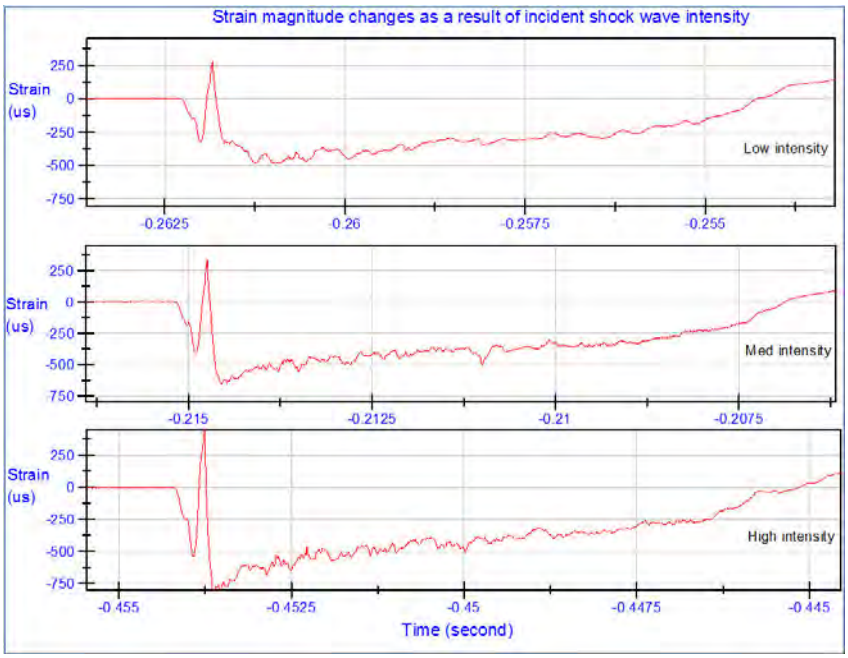

Figure 9: Strain magnitude as a result of incident shock wave intensity.

The strain data did prove to be useful for investigating the effect of orientation on the response of the PMHS head to an incoming shock wave. Two examples are provided in Figure 10 and Figure 11; the changes in response as a result of orientation are shown for the temporal sensor of PMHS #5 and the occipital channel of PMHS #3.

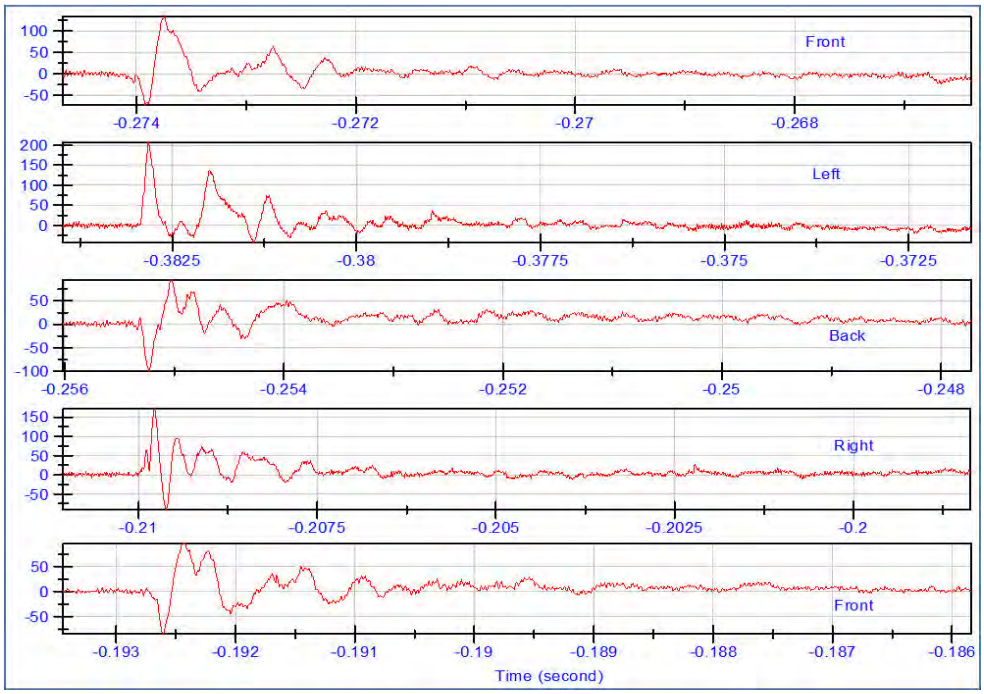

Figure 10: Strain data from the temporal bone for varying directions of shock wave exposure. Compression is positive and tension is negative.

As described prior, the PMHS specimen is placed in an inverted position in the shock tube. The temporal strain gage is adhered to the middle of the temporal bone surface on the left side of the head. In Figure 10, in the first exposure (front), when the shock wave traversed the head, a tension developed prior to a rapid compression. It is hypothesized that this tension is a surface wave that is propagated by the shock wave, which is acting as a moving load across the skull surface. The rapid compression would then be a result of the shock wave interacting with the bone surface. The oscillations that follow this deflection, which appears to act in a damped harmonic manner, would then be a result of the surface of the bone returning to equilibrium. In the second exposure, the head is rotated so that the temporal bone is facing the shock wave directly. In this event, the initial tension is not present but a rapid compression is. It is believed that this is a result of the incoming incident shock wave. When the head is rotated again, with the temporal bone perpendicular to the shock wave, the initial tension develops once again prior to the first compression. When the temporal bone is facing away from the event the waveform demonstrates a unique waveform where there are multiple oscillations that lead to the peak compression.

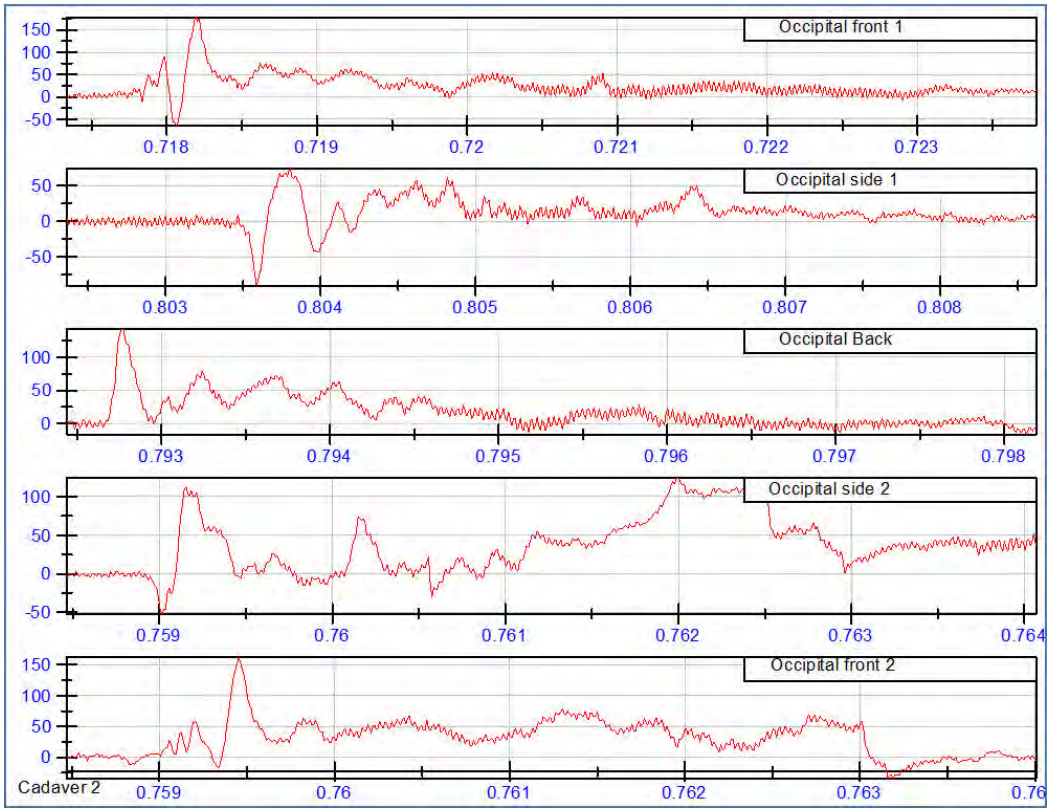

Figure 11: Strain seen in occipital bone with varying exposures. Compression is positive and tension is negative.

In Figure 11, when the head is facing forward, the occipital channel is facing away from the event. Figure 11 demonstrates that several oscillations developed prior to the major compression, which is similar to when the temporal bone was facing away from the event. When rotated, the tension wave prior to the major compression was evident for both occipital side 1 and 2, which is also similar to the results described for the temporal strain gage. When the

occipital bone was directly facing the incoming shock, a rapid compression would develop similar to the temporal channel.

We believe that there is a mode of skull deformation due to a global compression of the skull (Dal Cengio Leonardi et al. 2009). According to the thickness of the skull, what side of the head is facing the shock front, and the irregular geometry of the skull, deformation would create different patterns (profile shape) of pressure readings in relation to sensor location in the brain and to the forms of exposure. Due to geometry and specific material responses of the skull and its interfaces, some areas inside the brain could actually see a release of pressure prior to global compression. Figure 12 shows an example of the simultaneous recording of the 5 strain gages in one test.

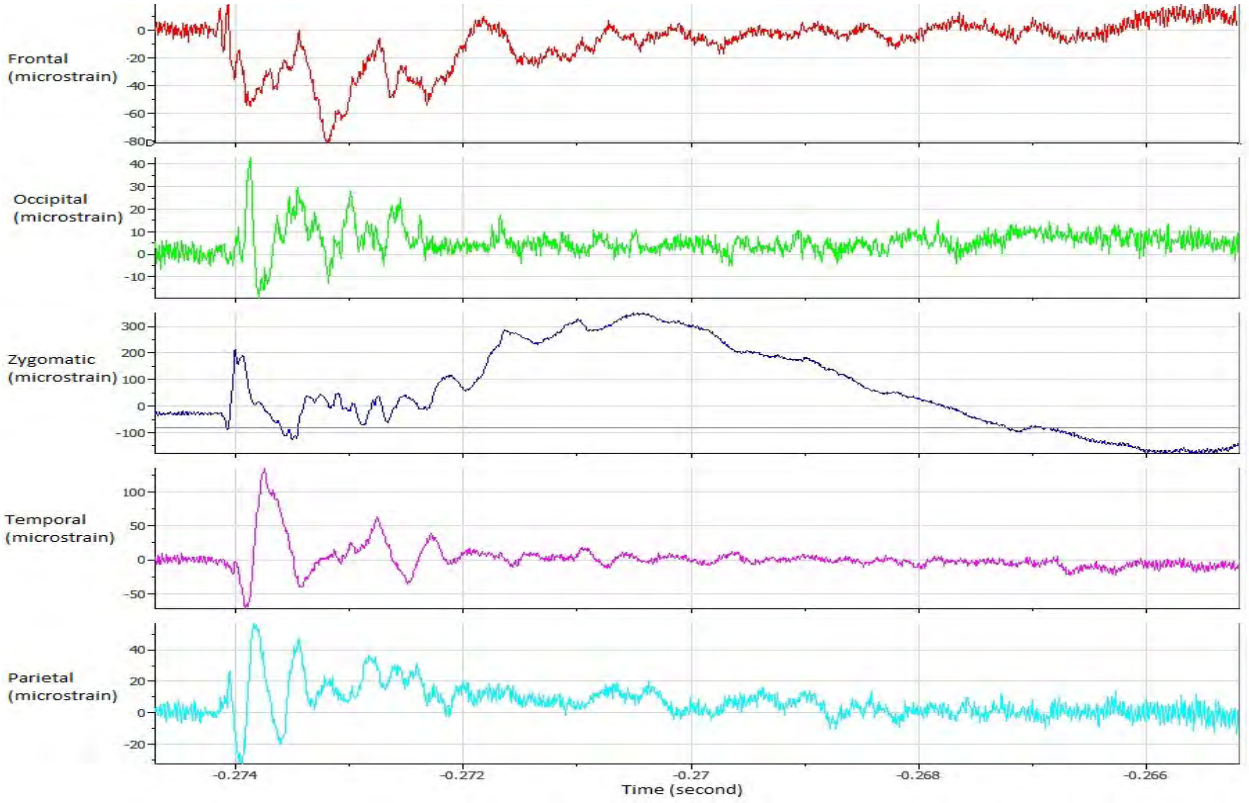

Figure 12: Strain data from frontal exposure, low intensity.

Task 3: Comparison of pressure distribution patterns with finite element (FE) model.

The final task of this work was to compare the experimental results with an existing FE model of the human head with detailed anatomical structures. The head model has been extensively validated and exercised for TBI prediction from blunt impact (Zhang et al. 2001).

The FE mesh of the WSU conical shock tube was developed using Hypermesh 9 preprocessor (Altair, Troy, MI) based on the actual geometry of the shock tube. To simulate the shock formation and wave propagation, the Smooth Particles Hydrodynamics technique (SPH) was originally proposed as a numerical technique to achieve the goal. However, in our recent study (Zhang and Sharma, 2009) it has been shown that SPH method suffers numerical solution

inaccuracy and computational efficiency problems due to strong dependency on the use of large number of particles. In Zhang and Sharma's study, a new coupled Multi-Material Arbitrary Lagrangian - Eulerian (MMALE) method was tested and applied successfully to predict the WSU head model responses to various blast exposures.

The method has been incorporated in the LS-Dyna, an explicit nonlinear, large deformation, dynamic finite element solver (LSTC, Livermore, CA). In the current study, MMALE algorithm was adopted to model high pressure chamber (driver), air chamber (driven) and the wave phenomena (wave propagation and formation of the shockwaves) within the WSU shock tube. The fluid dynamic characteristics of the helium and air were defined based on the published data. The driver pressures were simulated based on the actual pressure levels used in the PMHS experiments. The real-time recorded pressure sensor data at sensors named RWall and Sideon (pencil probe) were used to validate the simulation results.

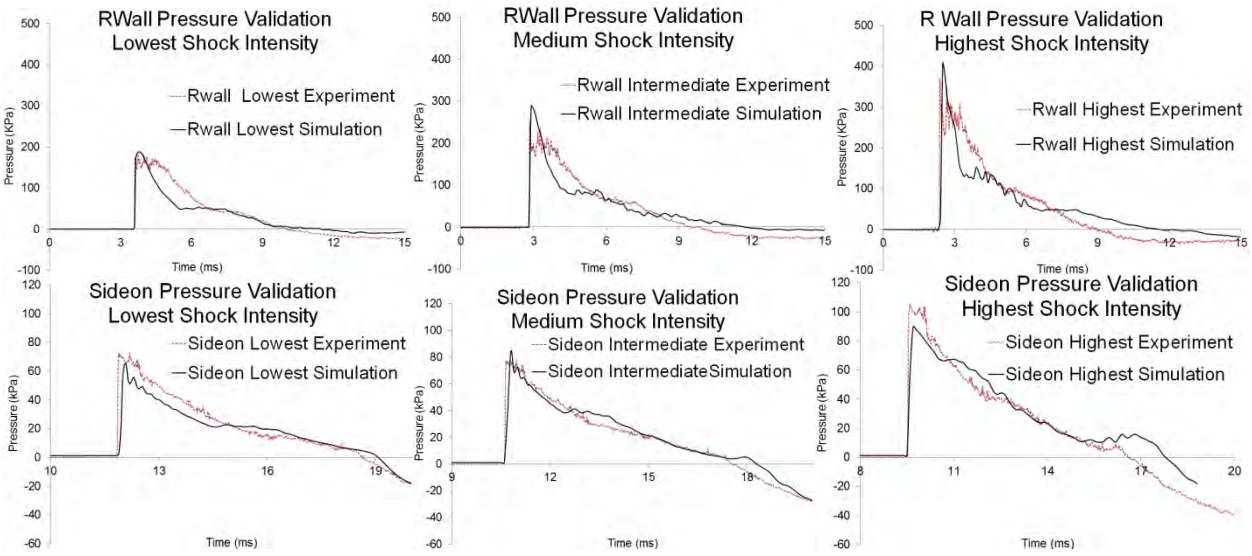

Figure 13 shows the comparison of the pressure time histories obtained at two locations between the model predictions and pressure sensor measurements. The model results agreed well with the sensor data in terms of peak pressure magnitude and overall pulse duration. At the RWall location, the pressure plateau after initial high spike was shorter in model results as compared to that measured from the tests. The cause of the discrepancy was unclear and requires further investigation. This discrepancy was not found in Sideon pressure validation. Figure 14 depicts the predicted overpressure profiles within the shock tube at different time points before impinging on the head model.

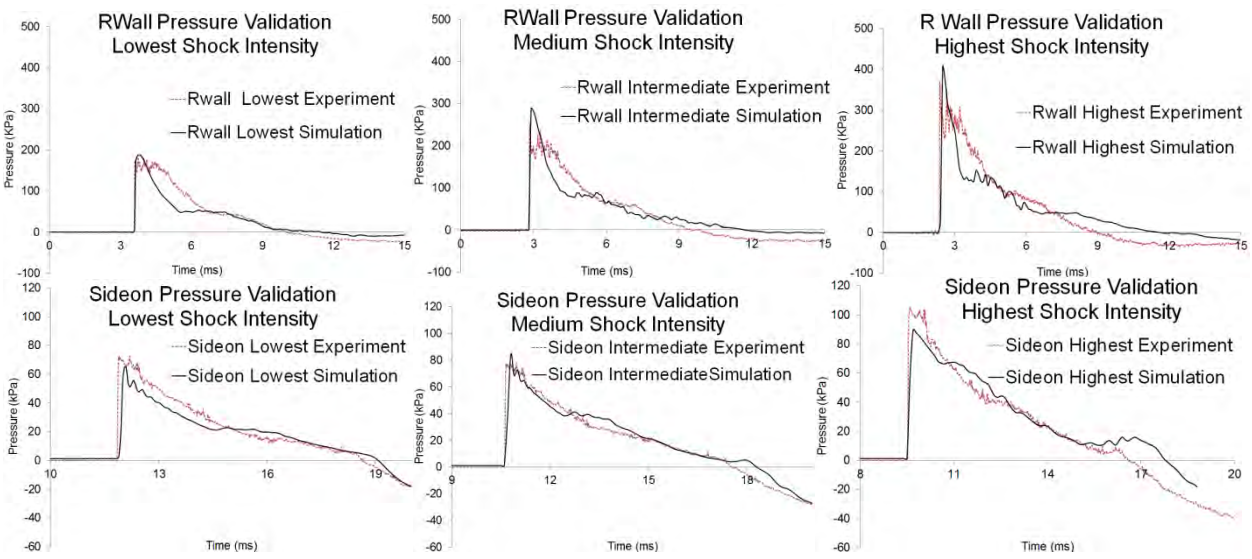

Figure 13: Comparison of the sideon pressures in the RWall and pencil at low, intermediate and high blast intensities between the model results and pressure sensor data measured during the actual experiments.

T = 6.5 ms T = 10.5 ms T = 12 ms

Figure 14: Pressure profiles in the shock tube at three time points after the bursting of the membrane between the driver and driven chambers

Simulation of the shock wave interaction with the head

In ALE method, the interaction between Eulerian and Lagrangian mesh is achieved using a Fluid Solid Interaction (FSI) coupling technique to transfer the momentum from blast wave to the structures upon receiving the shock load. The degree of the coupling depends greatly upon the mesh densities used between the Eulerian and Lagrangian models. The average mesh size of the WSUHIM head model is 2-3 mm. To ensure the proper coupling yet keep realistic computational cost, the numerical convergence study was conducted to compare the intracranial pressure response in the head model from the shock tube models meshed with different element sizes (20, 15, 10, 5, 3 mm).

The ICP induced in the head model from blast wave meshed at 10 mm was found to be within 10% differences in ICP results from 5 and 3 mm mesh. 10 mm mesh size significantly reduced the computational time and resources (> 100%) as compared to the finer meshed models. Therefore 10 mm mesh size was considered to be adequate to assure the energy transfer between two media.

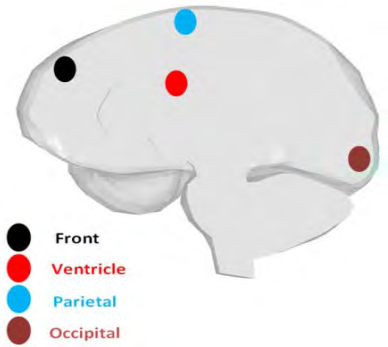

Validation of the intracranial pressure responses

The head model was positioned forward, backward and sideways with respect to the shock front coming through the

shock tube; the same configuration as the blast events used for the PMHS tests. At each head orientation, the model was exposed to three blast intensities at about 71 kPa, 76 kPa and 104 kPa, namely low, intermediate and high blast. The locations of the four pressure transducers, namely front (10 mm lateral to the midline, 30 mm in depth), parietal (10 mm lateral to the midline, 30 mm in depth), occipital (5 mm lateral to the midline, 30 mm in depth) and ventricle, within the brain of the PMHS were defined for the head model at the corresponding locations (Figure 15). The time histories of intracranial pressures responses predicted by the models at these locations were compared to those measured from the pressure sensors to validate the FE model in response to given shock waves. It was noticed that some of the sensor measurements in some of the PMHS tests were not reliable. Therefore only PMHS #4 and #5 results were used for model comparison for all simulated cases.

Figure 15: The location of the elements defined in the WSUHIM for output of the pressure responses.

Forward blast: Figure 16 shows the comparison of the pressure time histories between model simulations and experimental measurements in forward blast loading condition. In general, the model predicted pressure patterns/trends in the frontal brain matched the overall experimental results. The peak values of pressure magnitudes however were under-predicted by the model at three blast intensities. This was likely related to the discrepancy between the model and PMHS in terms of the Frankford plane in relation to the blast direction. This orientation difference may cause dissimilarity in incidence angle, which, in turn, is inducing varying amount of reflected and transmitted blast wave to the frontal region of the brain. For ventricular pressure, model predictions seemed to fall within the two PMHS data for the low and intermediate blast. At the high blast level, the model predicted ventricular pressure was higher along with a longer duration for the positive phase than the PMHS responses. The parietal pressure measured from PMHS #4 and #5 had reverse trends. The model results, however, had some degree of correlations to that of PMHS #5 results. For occipital pressure, the model results matched PMHS #4 in terms of peak magnitudes whereas in terms of pressure duration responses the model results fell between the two PMHS measurements.

Sideways blast: Figure 17 shows the comparison of the peak pressure between the model predictions and available PMHS results at all locations in response to both sideways and backward blast loadings. In sideways blast, the model predicted parietal pressure (coup) matched well with the PMHS data at the same regions. The ventricular pressure predicted by the model matched PMHS #5 results but over-predicted for the averaged values of two PMHS (#4 and #5). Notice that the significant difference was found between these PMHS data measured at the same locations.

Backward blast: In backward PMHS tests, occipital sensor data were available only for PMHS #5 not for PMHS #4. Based on the comparison as shown in Figure 17, the model predicted higher occipital and frontal pressure than that measured in PMHS #4 but lower pressure in the front (contrecoup) than in PMHS #5. By looking at the measured pressure values in the frontal region (contrecoup) between the PMHS #4 and #5, one would expect a much higher coup pressure in PMHS #5 than in PMHS #4. More completed and repeatable experimental data are needed before the FE model can be rigorously validated at all conditions.

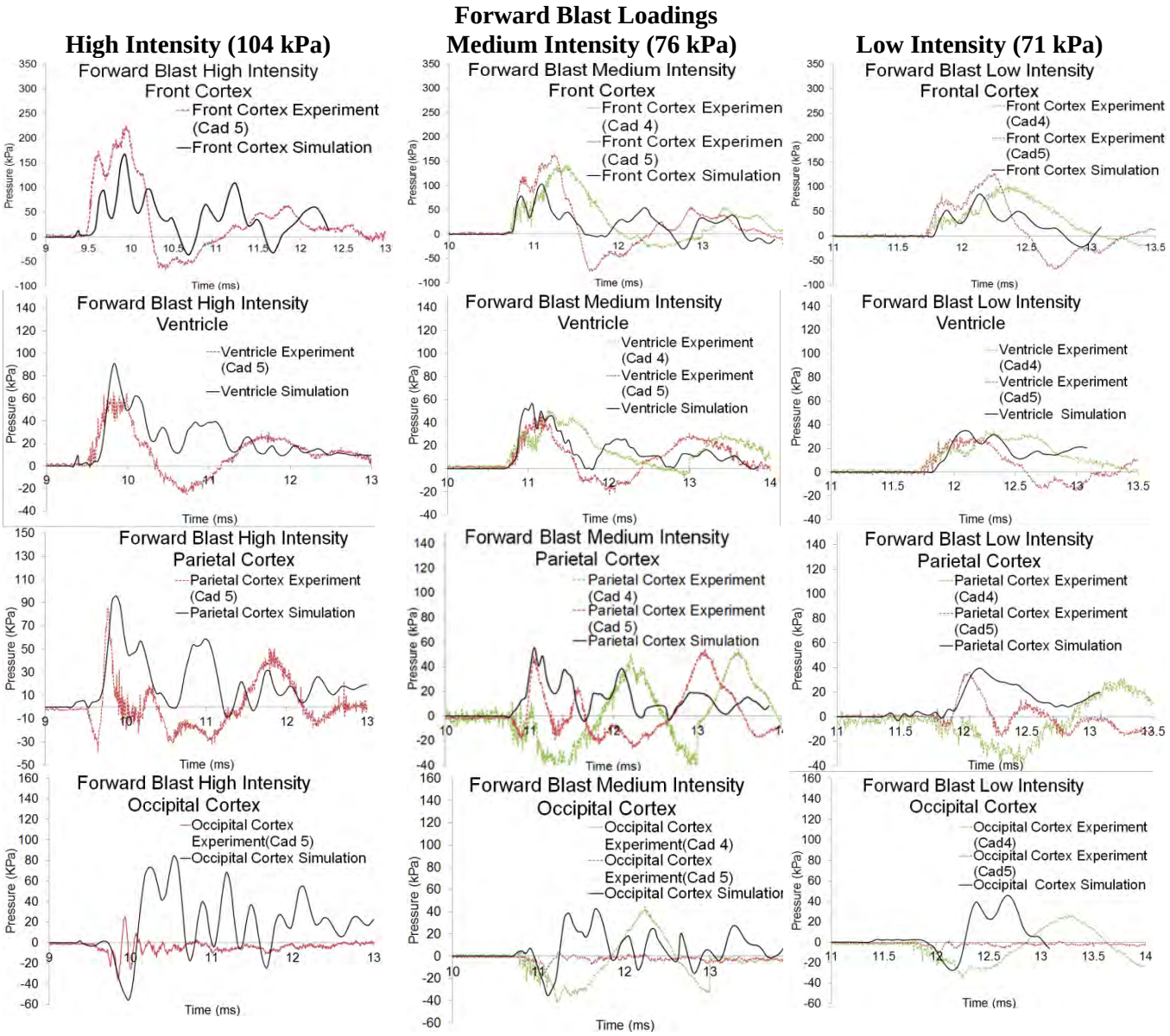

Figure 16: Validation of the ICP at the frontal, parietal, occipital and ventricle regions as results of forward blast loadings of three intensities.

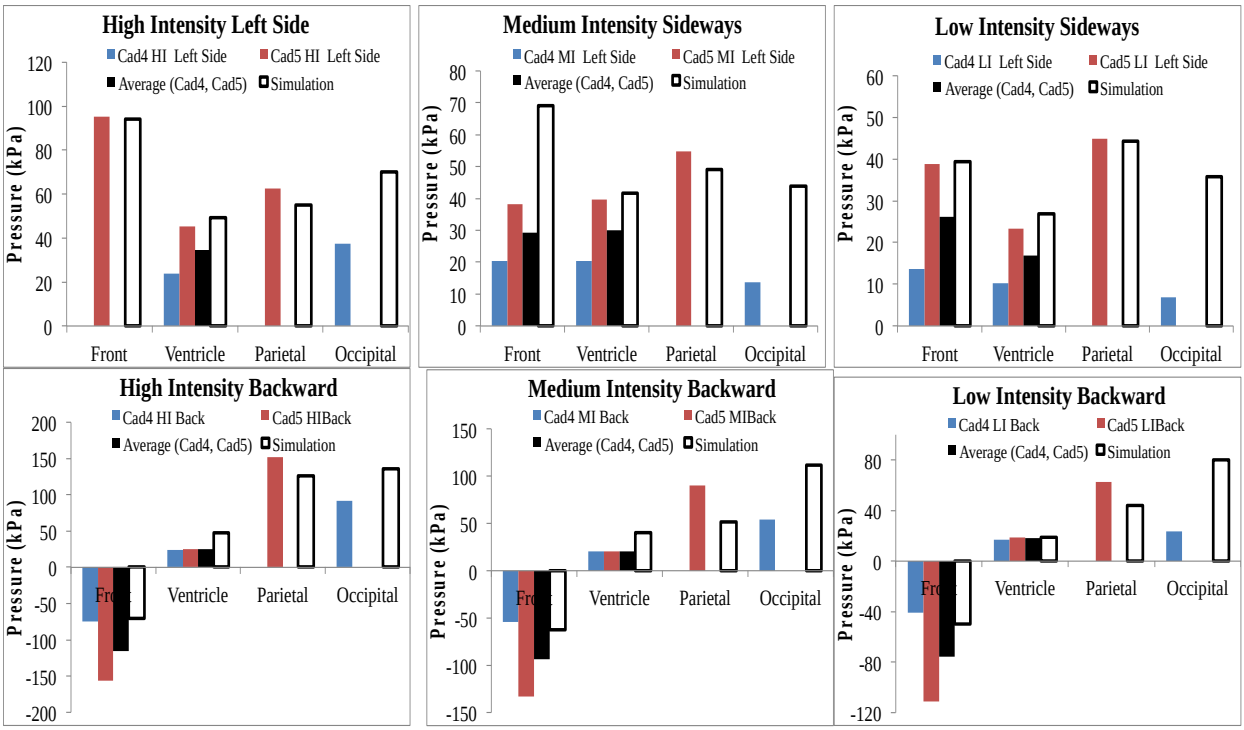

Figure 17: The ICP peak values predicted by the model in the frontal, parietal, occiptal and ventricle regions were compared to the sensor data measured from PMHS #4 and #5 and their average results in case of sideways blast and backward blast at all three intensities.

The blast wave propagation within the shock tube and wave interaction with a high resolution human head model were successfully simulated using finite element techniques utilizing a coupled Eulerian-Lagrangian method to understand the dynamic and biomechanical response of the human brain subjected to blast loading. The finite element model of the human head (WSUHIM) was then validated against experimentally measured PMHS intracranial pressure in the brain from three different head orientations at three different blast severities which has never been described or reported previously. The pressure profile predicted by the FE model both in terms of temporal and spatial patterns generally agreed with those of experimental results. The model and PMHS ICP-results appeared to be correlated better in the forward and sideways blast condition than the backward blast conditions. More completed and repeatable experimental data are needed to rigorously validate FE model in various blast environment.

From the model validation studies, the simulation results demonstrated that the pressure wave was directly coupled with the brain at about 2 times higher than the air overpressure (sideon pressure). The brain facing the oncoming blast front always sustained higher pressure than the other regions of the brain. Coup and contrecoup phenomena were observed in all cases.

Future work should incorporate animal experiments of blast injury with animal modeling to determine the tissue level biomechanical estimates with pathophysiological outcomes of blast TBI. Such defined tissue level threshold information once translated to a valid human head model will enable the biomechanical head model to be used as a design tool to improve the blast protection for our soldiers.

KEY RESEARCH ACCOMPLISHMENTS

- Determination that pressure sensor location has a major role in pressure measurements.
- Determination that the strains seen in the skull are dependent on the orientation of the shock wave exposure.
- Development of a preliminary FEM that show initial correlation with the experimental results.

REPORTABLE OUTCOMES

The following PhD Thesis was completed as part of this effort:
"An investigation of the biomechanical response from shock wave loading to the head" by Alessandra Dal Cengio Leonardi. PhD defense April 25th, 2011.

The following presentation of data was given as a part of this effort:
"Measuring Blast-Related Intracranial Pressure within the Human Head" by Bir and VandeVord. The Third DOD Blast Injury State-of-Science Meeting. Dec 2010

The following abstract were submitted as a part of this effort:
"A Biomechanical Prospective of Blast Injury Neurotrauma" by Bir, Bolander, Leonardi, Ritzel and VandeVord, Submitted to the NATO HFM 207 Symposium

The following personnel were supported through this funding: Cynthia Bir (Professor - partial summer salary), Richard Bolander (Graduate Student – partial PhD funding), Nathan Dau (research assistant – partial funding), James Kopacz (research assistant), Pamela VandeVord (Associate Professor - partial summer salary), Bin Wu (research assistant – partial funding) and Liying Zhang (Research Professor – partial funding)

CONCLUSION

In conclusion, we demonstrated that there are significant factors of paramount importance when performing ICP-PMHS testing: sensor location in the brain, exposure at blast, orientation of head and magnitude of the blast. There is a pressing need for a comprehensive explanation of the mechanism of traumatic brain injury after exposure to blast, and the testing of instrumented PMHS specimens will become increasingly important. Historically, some animal tests have been designed and carried out in an attempt to learn more about the mechanism of shock wave transmission to the brain, but only a few animal studies recorded direct pressure within the brain tissue during exposure to blast (Clemedson 1956; Clemedson and Jonsson 1961; Romba and Martin 1961; Chavko et al. 2007; Saljo 2008; Dal Cengio Leonardi et al. 2009; Dal Cengio Leonardi et al. 2011). In fact such experiments are challenging to setup because animal tests carry the burden of the complex preparation of the animals in addition to the strict guidelines for animal handling. It is of paramount importance to conduct tests in a way that will maximize the attainment of dependable results and minimize the sacrifice of animals: by using PMHS specimens we combined these to the advantage of working with the human unique geometry.

REFERENCES

Celander, H., Clemedson, C.J., Ericsson, U.A., Hultman, H.I. (1955). "The use of a compressed air operated shock tube for physiological blast research." Acta Physiologica Scandinavica 33(1): 6-13.

Chavko, M., Koller W.A., Pruzaczyk W.K., McCarron R.M. (2007). "Measurement of blast wave by a miniature fiber optic pressure transducer in the rat brain." Journal of Neuroscience Methods 159(2): 277-81.

Clemedson, C.J. (1956). "Shockwave transmission to the central nervous system." Acta Physiologica Scandinavica 37(2-3): 204-14.

Clemedson, C.J., Jonsson, A. (1961). "Transmission of elastic disturbances caused by air shock waves in a living body." Journal of Applied Physiology 16(3): 426-430.

Dal Cengio Leonardi A., Bir C.A., Ritzel D.V., VandeVord P.J. (2009). "The effects of intracranial pressure sensor location and skull apertures during exposure of a rat model to an air shock wave." The Second Joint Symposium of the International and National Neurotrauma Societies, Santa Barbara, CA, Poster Presentation, September 2009.

Dal Cengio Leonardi A., Bir C.A., Ritzel D.V., VandeVord P.J. (2011). "Intracranial pressure increases during exposure to a shock wave." Journal of Neurotrauma 28: 1-10.

Romba, J.J., Martin, P. (1961). "The propagation of air shock waves on a biophysical model." Armed Services Technical Information Agency, Arlington Hall Station, Arlington 12, Virginia. U.S. Army Ordnance. Technical Memorandum 17-61. Human Engineering Laboratories, Aberdeen Proving Ground, Maryland: 1-25.

Saljo, A., Arrhen, F., Bolouri, H., Mayorga, M., Hamberger, A. (2008). "Neuropathology and pressure in the pig brain resulting from low-impulse noise exposure." Journal of Neurotrauma 25: 1397-1406.

Zhang, L., Yang, K. H., King, A. I. (2004). "A proposed injury threshold for mild traumatic brain injury" Journal of Biomechanical Engineering, 126(2): 226-236.

Zhang L, Sharma S. (2009) “Computational modeling of causal mechanisms of blast wave induced traumatic brain injury – a potential tool for injury prevention”, Technical Progress Report, Department of Defense, Washington DC.